Northward range expansion of Bay of Biscay anchovy into the English Channel

Jeroen van der Kooij[1,*], Niall McKeown[2], Fabio Campanella[1,6], Guillermo Boyra[3],
Mathieu Doray[4], Maria Santos Mocoroa[3], Joana Fernandes da Silva[1], Martin Huret[5]

[1]Centre for Environment, Fisheries and Aquaculture Science, Pakefield Road, Lowestoft NR33 0HT, UK
[2]Aberystwyth University, Institute of Biological, Environmental and Rural Sciences (IBERS), Aberystwyth SY23 3DA, UK
[3]AZTI, Marine Research, Basque Research and Technology Alliance (BRTA), Herrera Kaia,
Portualdea z/g, 20110 Pasaia (Gipuzkoa), Spain
[4]DECOD, L'Institut Agro, IFREMER, INRAE, 44311 Nantes, France
[5]DECOD, L'Institut Agro, IFREMER, INRAE, 29280 Plouzané, France

[6]*Present address:* National Research Council (CNR), Institute for Biological Resources and Marine
Biotechnologies (IRBIM), Largo Fiera della Pesca, 2, 60125 Ancona, Italy

ABSTRACT: European anchovy *Engraulis encrasicolus* is a widely distributed, warm-water species which has been postulated to be a climate change 'winner'. For decades, the northern-most stock resided in the Bay of Biscay, where it typically spawned during late spring, mostly in the south. An apparent regime shift in the mid-1990s saw the sudden appearance and subsequent increase of anchovy further north. This northward range expansion was found to be driven by remnant spawning populations in the North Sea. During the autumn of 2019 and 2020, for the first time, post-larval anchovy were found in the English Channel, far from their nearest known spawning grounds. Identifying the origin of these anchovy is important for management purposes and to understand the mechanisms driving populations at the limits of their distribution. Microsatellite- and mtDNA-based analyses confirmed that the observed post-larval anchovy originated from the Bay of Biscay and were genetically distinct from English Channel and southern North Sea specimens. By combining acoustic and egg data from local surveys with larval drift modelling, we examined the processes underpinning this northward expansion. Our analysis suggests that due to population increase, spawning activity in the Bay of Biscay has expanded in space and time, increasing larval transport and survival into the Channel area. This newly recorded process underpinning an observed pole-ward shift is different from the one driving the anchovy expansion that started in the mid-1990s. However, both caused range expansion at the species' northern distribution limit, demonstrating the potentially complex impacts of climate change.

KEY WORDS: *Engraulis encrasicolus* · Climate change · Connectivity · Acoustics · Population genetics · Larval drift modelling · Spatial density-dependent effects

1. INTRODUCTION

Understanding species distributions is important for management and conservation purposes. Species distributions are expected to change substantially due to climate change, with shifts in the limits of the distribution ranges (Pinsky et al. 2020), even more rapidly in the oceans than on land (Lenoir et al. 2020). Investigating the mechanisms underpinning observed contractions and expansions and changes in phenology will aid in predicting any future changes as a result of ecological or anthropogenic drivers (Pörtner & Peck 2010). Climate change affects lower trophic levels such as phytoplankton (Boyce et al. 2010) and zooplankton (Ratnarajah et al. 2023 and references therein), with cascading impacts on higher trophic levels. Small pelagic fish exhibit large changes in abundance and distribution. This is because they

respond rapidly to changing environmental conditions as they are short-lived, exhibit rapid growth and high fecundity and depend directly on zooplankton prey. Although statistical projections of small pelagic fish distribution in Europe predict significant expansion to the north (Schickele et al. 2021), the mechanisms driving these changes vary by species, and are often poorly understood (Peck et al. 2021).

European anchovy *Engraulis encrasicolus* is a widely distributed warm-water species which is found from South Africa northwards along the shelf seas of west Africa into the Mediterranean and Black Seas and in northwestern European waters (Kaschner et al. 2019). Here, it is generally considered a climate change 'winner' (Townhill et al. 2023), and the Bay of Biscay (Fig. 1) has traditionally represented its most consistent northern-most spawning area. The Bay of Biscay stock is of significant commercial importance, and as part of its management, the fishery was closed between 2005 and 2009, following a succession of poor recruitments. Since 2010, when the fishery reopened, the stock has continued to rebuild with the highest historical biomass observed in recent years (ICES 2023). The reasons for this increase seem to be a combination of good recruitment linked to favourable environmental conditions and a reduction in fishing mortality (Bueno-Pardo et al. 2020, Uriarte et al. 2023).
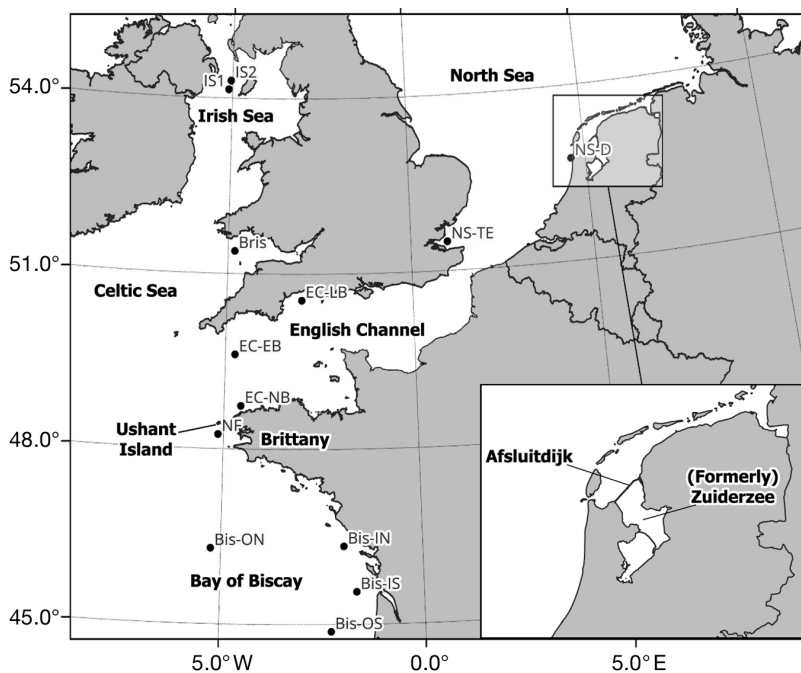

Fig. 1. Study area in the Northeast Atlantic Ocean, including North Sea, English Channel, Bay of Biscay and other relevant geographic areas as referenced in the text, including the historic Zuiderzee (inset). Genetic sampling stations denoted by black points (•), with associated details, including location names, given in Table 2

Historically, spawning did occur farther north in the Zuiderzee (Fig. 1), a shallow inland sea off the southern North Sea. Anchovy were reportedly found in significant numbers (Aurich 1953), until in 1932, the Zuiderzee was sealed off from the North Sea following the introduction of a dam (the Afsluitdijk, Fig. 1) and anchovy all but disappeared from the area for decades (Beare et al. 2004a). From the mid-1990s, increasing numbers of anchovy were reported from the northern fringes of its traditional distribution: from opportunistic commercial landings in the English Channel, and from catches in fisheries-independent surveys in the Irish Sea (Armstrong et al. 1999) and particularly the North Sea (Boddeke & Vingerhoed 1996, Beare et al. 2004a,b, Alheit et al. 2012, Montero-Serra et al. 2015). In the absence of dedicated anchovy surveys in key areas, a collaborative multidisciplinary approach aimed to determine the origin of these anchovy in the North Sea and the possible mechanisms underpinning their increase (Petitgas et al. 2012). North Sea anchovy were found to be genetically distinct from those in the Bay of Biscay. Further evidence of a lack of connectivity with the Bay of Biscay was provided by the results of a particle drift modelling experiment, which confirmed that eggs released from the main spring-spawning locations situated in the southern part of the Bay of Biscay were unlikely to reach the North Sea or the English Channel (Petitgas et al. 2012). While limited spawning did occur in the north of the Bay of Biscay, it occurred later in the season, when prevailing hydrographic circulation was more southward, which would also have prevented anchovy from reaching the English Channel and the North Sea. The study therefore provided strong evidence that the observed increase of anchovy in the northern part of its range was due to improved recruitment of a local remnant population rather than a colonisation of the North Sea by Bay of Biscay anchovy as eggs/larvae or as adults (Petitgas et al. 2012).

From 2013, a new pelagic survey provided the first fisheries-independent information on anchovy in the western English Channel, directly north of the Bay of Biscay (PELTIC survey, Doray et al. 2021). The survey took place during the autumn, when North Sea-spawned anchovy migrate to the

western English Channel (Huret et al. 2020) and appear as opportunistic bycatch in some of the local sardine and sprat fisheries. Anchovy were found in the English Channel from the start of the survey series (2013), first in small numbers but annually increasing in both range and biomass (ICES 2021). Biological data confirmed that anchovy of different ages, including age 0, migrate from the North Sea to overwinter in the English Channel, as previously reported (Petitgas et al. 2012, Huret et al. 2020). In the early years of the survey, anchovy were only found in mixed aggregations with other small pelagic species. More recently, as anchovy biomass increased, monospecific schools became more common and were typically found in the lower half of the water column.

During the 2019 and 2020 PELTIC surveys, a new observation suggested potentially further changes to anchovy dynamics. For the first time, post-larval anchovy were observed as surface schools along the transects off the north coast of Brittany (France). The unusual shape and behaviour of the surface schools (Fig. 2), resembling post-larval or juvenile anchovy from the Bay of Biscay (Boyra et al. 2016), and their geographic position, seemingly emerging from the southwest of the English Channel and extending east along the Brittany coast, suggested that these anchovy were different from those typically encountered in the area. Given that the English Channel appears to be a natural boundary between 2 spawning populations, i.e. Bay of Biscay anchovy in the south and the North Sea population further northeast (Petitgas et al. 2012, Huret et al. 2020), it is important to identify the origin of these anchovy and the possible reason for this change.

We used 3 different approaches to investigate the possible causes behind these observations. Firstly, the origin of the anchovy juveniles was investigated using genetics, through individual assignment (IA) tests. Specifically, adults collected throughout the Bay of Biscay, English Channel and North Sea regions were genotyped at microsatellite loci to establish the genetic characteristics of the southern (Bay of Biscay) and Northern (Channel/North Sea) populations. This differentiation then permitted individual post-larvae to be assigned to their respective source population. Secondly, any recent changes in annual anchovy juvenile and egg distribution were investigated by comparing them with historic distribution maps from fisheries-independent surveys in the broader area. Thirdly, the potential roles of regional oceanographic processes underpinning these observations were explored. A particle tracking model was used to investigate any recent changes in the connectivity patterns from the observed spawning locations, which may be able to explain the observations in 2019 and 2020. Also, the potential role of the Ushant Front, an important seasonal hydrographic feature located between the Bay of Biscay and the English Channel
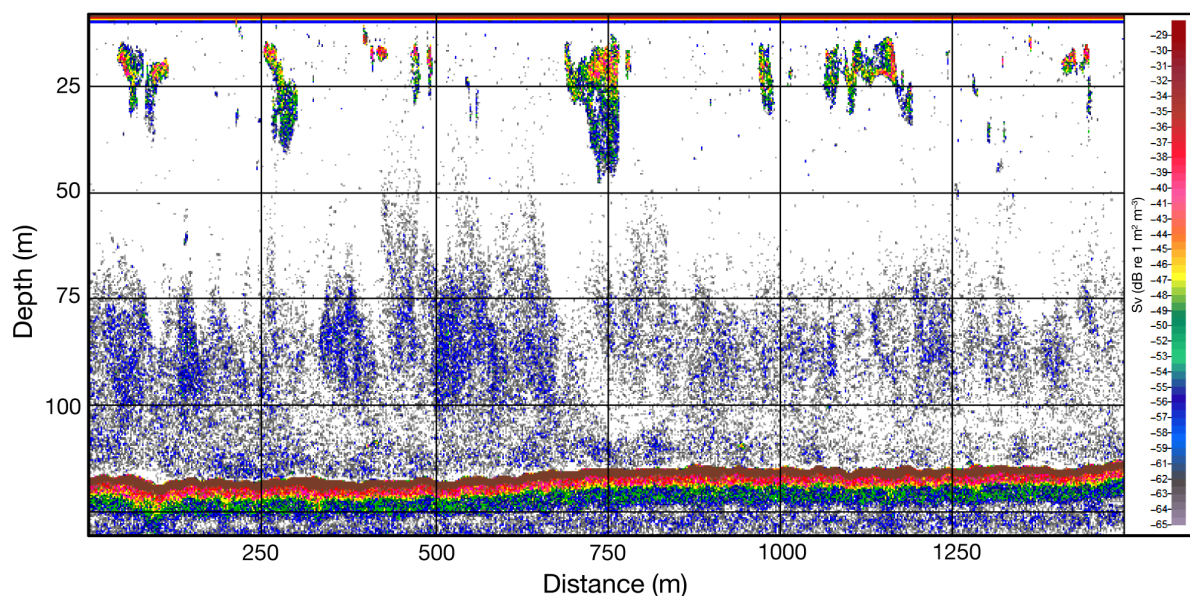

Fig. 2. Echogram (visualised using Echoview Software®) displaying an example of post-larval/juvenile anchovy surface schools observed during the PELTIC survey in French waters of the western English Channel. This example was observed on 18 October 2020 at 10:41 h GMT and was representative of post-larval observations in 2019 and 2020. Echogram represents backscatter at 38 kHz (density scale on right) and −65 dB threshold. Depth (m) on *y*-axis (top to bottom), and distance (m) on *x*-axis. Seabed is represented by dense (red/brown) layer at bottom

(Pingree 1975), was investigated. Fronts may act as a barrier to cross-frontal mixing of planktonic organisms (Woodson et al. 2012), and interannual variation in the autumn position of this front was explored using temperature profiles recorded during the PELTIC surveys.

2. MATERIAL AND METHODS

2.1. Surveys

Data on anchovy eggs, juveniles and adults formed the basis of this study and were collected on several annual pelagic surveys in the Bay of Biscay and the western English Channel. All surveys considered in this study were annually coordinated, which includes standardisation of methodologies (Doray et al. 2021). A detailed description of the surveys is provided elsewhere (Doray et al. 2021) and a short summary is included here (Table 1). These data were included to explore the wider distribution and connectivity of anchovy juveniles in the Bay of Biscay and western English Channel during the autumn and the associated spawning location in the preceding spring.

2.2. Genetics

2.2.1. Sample collection and molecular analyses

Samples of adult anchovy were collected from a number of sites across multiple years by demersal and pelagic trawls (Table 2, Fig. 1). All samples contained multiple age classes apart from the 2019 sample, which consisted solely of juvenile anchovy. Individual (dorsal) finclip samples were preserved in absolute ethanol. Genomic DNA was extracted using a standard cetyltrimethyl ammonium bromide (CTAB)-chloroform/isoamylalcohol method (Winnepenninckx

et al. 1993). Nuclear variation was assessed at 6 microsatellite loci: Ee2, Ee10 (Landi et al. 2005), Ee2-91b, Ee2-135, Ee2-507 and Ee2-508 (Pakaki et al. 2009). The various loci were individually amplified by PCR in 10 µl reactions containing ~50 ng of DNA, 3 pmol of each primer (forward primer labelled with a Cy5 fluorescent dye group), 0.1 U of *Taq* DNA polymerase (Bioline), 1× supplied PCR Buffer, 2.0 mM $MgCl_2$ and 0.2 mM deoxynucleotide triphosphate (dNTP) and using the originally described thermoprofiles for each locus. PCR amplicons were separated on an Applied Biosystems 3500 sequencer with alleles inferred using GENEMAPPER (Applied Biosystems). mtDNA sequence variation was assessed by PCR amplification of the control region using primers described by Pappalardo et al. (2015) and sequencing using the internal primer (5'-CCC TTA GGC AGT TCA AGC AC-3') with Big Dye technology on an Applied Biosystems 3500. Sequence alignment was performed in BioEdit (Hall 1999) using default settings.

2.2.2. Statistical analysis of genetic variation

Microsatellite variation within samples was characterised using numbers of alleles (N_A), allelic richness (A_R), observed heterozygosity (H_o) and expected heterozygosity (H_e), calculated using FSTAT 2.9.3 (Goudet 1995). Deviations from Hardy-Weinberg equilibrium (HWE) were measured using F_{IS} and tested for significance by 10 000 permutations in FSTAT 2.9.3, while genotypic linkage equilibrium between pairs of loci was tested using exact tests (10 000 batches, 5000 iterations) in GENEPOP 3.3 (Raymond & Rousset 1995). Genetic differentiation among samples was quantified by global and pairwise F_{ST} values, with associated significance evaluated by 10 000 permutations (exact F_{ST} estimator test, Goudet et al. 1996). Pairwise F_{ST} values among samples were visualised using principal coordinates analysis, performed in genetic analysis in Excel (GenAlEx). mtDNA varia-

Table 1. Summary details of relevant fisheries-independent surveys in the Northeast Atlantic Ocean that collect data on anchovy. CUFES: Continuous Underway Fish Egg Sampler. Where available, data from the years 2008−2010 and 2017−2021 were used in this study. More details are provided in the survey manual (Doray et al. 2021)

Survey	Geographic area	Season	Timeseries start	Data used in this study
PELGAS	Bay of Biscay	April−May	2000	Anchovy eggs (CUFES)
BIOMAN	Bay of Biscay	May	1987	Anchovy eggs (CUFES)
JUVENA	Bay of Biscay	September	2003	Anchovy juveniles (acoustics)
PELTIC	Celtic Sea/English Channel	October	2013	Anchovy adults, juveniles (acoustics) and fish eggs (ringnet)

Table 2. Sample information including sample sizes for both mtDNA and nuclear microsatellite analysis. For mtDNA, the number of haplotypes (nHap) and haplotype diversity (*h*) per sample, and the abundances of the 2 clades (A and B) are reported. For microsatellites, the mean number of alleles (N_A) and allelic richness (A_R), as well as observed (H_o) and expected heterozygosities (H_e) and F_{IS} values (values significant at p ≤ 0.05 denoted by *) are reported

Sample site	Code	Coordinates	Date	Sample size mtDNA/ nuclear	nHap/*h*	Clade frequency (A:B)	Mean N_A/A_R	H_o/H_e/F_{IS}
Irish Sea-1	IS1	54.15° N, 5.11° W	March 2010	21/21	19/1	21:0	10/9.8	0.79/0.79/0.005
Irish Sea-2	IS2	54.30° N, 5.05° W	March 2011	13/80	13/1	13:0	14.8/10.5	0.75/0.84/0.115*
Bristol Channel	Bris	51.39° N, 4.82° W	Nov 2010	14/37	12/0.98	14:0	12.5/10.9	0.70/0.82/0.153*
English Channel —Eddystone Bay	EC-EB	49.62° N, 4.7° W	Nov 2010	16/74	14/0.98	13:3	15/10.1	0.73/0.80/0.089*
English Channel —Lyme Bay	EC-LB	50.55° N, 2.99° W	Nov 2010	14/72	11/0.96	14:0	14.5/10.4	0.69/0.82/0.166*
North Sea —Thames Estuary	NS-TE	51.5° N, 1° E	June 2011	10/73	10/1	10:0	14.8/10.4	0.71/0.83/0.140*
North Sea — Dutch	NS-D	52.75° N, 4.6° E	April 2011	13/53	10/0.92	12:1	11.7/9.3	0.70/0.82/0.150*
North France	NF	48.25° N, 5.14° W	Nov 2015	22/96	20/0.99	8:14	19.5/12.0	0.75/0.82/0.087*
Biscay inshore North	Bis-IN	46.34° N, 1.95° W	May 2011	14/75	12/0.98	6:8	17.8/11.3	0.76/0.81/0.063*
Biscay offshore North	Bis-ON	46.30° N, 5.25° W	May 2011	36/97	22/0.95	24:12	18.3/11.3	0.75/0.82/0.080*
Biscay inshore South	Bis-IS	45.56° N, 1.65° W	May 2010	16/60	14/0.98	8:8	13.5/10.1	0.73/0.78/0.065*
Biscay offshore South	Bis-OS	44.88° N, 2.28° W	April 2010	15/72	15/1	5:10	16/10.5	0.74/0.79/0.070*
English Channel-post larvae	EC-NB	48.74° N, 4.57° W	Oct 2019	47/48	38/0.98	34:13	16/11.2	0.74/0.79/0.070*

tion was described by haplotype number and haplotype diversity (*h*) (Nei 1978) calculated in Arlequin software (Excoffier & Lischer 2010). Phylogenetic relationships among haplotypes were inferred using maximum likelihood trees constructed in MEGA v 6.06 (Tamura et al. 2013). Partitioning of variation was analysed using analysis of molecular variance (AMOVA; Excoffier et al. 1992) derived estimates of various Φ-statistics, as well as pairwise $Φ_{ST}$ with significance of the various indices assessed by 10 000 permutations.

2.2.3. Assignment of post-larval anchovy individuals

The individual clustering method in STRUCTURE 2.3.4 (Pritchard et al. 2000) was used to estimate the most probable number of genetic groups within the data and the membership of individuals to these groups. Optimal models were assessed following Pritchard et al. (2000), and where there was support for *K* >1, Δ*K* (Evanno et al. 2005) was also assessed. To complement the individual-based STRUCTURE analysis, classical IA tests were also performed in GenAlEx. Specifically, the adult samples were pooled into Southern and Northern groups identified by F_{ST} and STRUCTURE analysis, which were then used as baseline samples in IA tests. The post-larval samples

were treated as 'unknown', and each individual was assigned to either the Northern or Southern group.

2.3. Anchovy egg and juvenile distribution

Dedicated anchovy data were available for the western English Channel from an acoustic autumn survey from 2017 (PELTIC survey; our Table 1; Doray et al. 2021), and the distinct acoustic backscatter data attributed to juvenile anchovy were combined with those from the Bay of Biscay (JUVENA survey; our Table 1; Boyra et al. 2013) to provide broad-scale distribution maps to explore any continuity in distribution of juvenile anchovy between the 2 areas. Acoustic backscatter collected during both acoustic surveys was partitioned by species and size using ratios obtained from nearby trawl hauls, although acoustic features such as school morphology also contributed (more details provided by Doray et al. 2021). As mentioned previously, the juvenile anchovy schools focused on in this study were different from the anchovy typically encountered during the PELTIC survey, and the species and size composition obtained from targeted trawls confirmed this.

We compared recent juvenile anchovy distribution maps from 2017—2021 to those from 2008—2010 as representative of a period of typical historical con-

ditions. Data from before 2008 were not considered, as the Bay of Biscay anchovy stock was recovering from a collapse following years of poor recruitment, which may not have been representative for historical observations. Unfortunately, no concurrent survey data were available for the English Channel for 2008–2010, but particle tracking modelling showed that eggs or larvae were unlikely to have made it to the English Channel in that period (Petitgas et al. 2012).

As changes in the juvenile anchovy autumn distribution may have been related to spawning location, we mapped anchovy egg density distribution for these same periods, 2008–2010 and 2017–2021. Anchovy egg data were available from 2 spring surveys, including PELGAS, (which collects information on egg densities using the Continuous Underway Fish Egg Sampler [CUFES, Checkley et al. 1997] whilst running acoustic transect lines), and the BIOMAN survey (Santos et al. 2018, 2023) (which collects information on egg densities using different methods including CUFES to sample eggs). Ichthyoplankton samples, including eggs and larvae, were also collected in the English Channel during the autumn, using a vertical ringnet deployment at up to 100 stations per year (Doray et al. 2021). Due to differences in sampling gears, survey design and data units (primarily acoustic and ichthyoplankton data), the spatial data were standardised by gridding the backscatter and egg density data (sensu Doray et al. 2018a) by 0.25° longitude and latitude cells.

2.4. Early life stage dispersal model

We used the Lagrangian particle tracking module detailed by Huret et al. (2010) to simulate the transport of early life stages of anchovy over the years 2008–2010, and 2017–2021 from known spawning grounds in the Bay of Biscay. The objective of simulating the early years was to test the hypothesis that no, or negligible, drift from the Bay of Biscay to the English Channel occurred compared to more recent years. We also simulated 5 recent years to check whether the simulated interannual variability in connectivity between the 2 eco-regions is consistent with our (field) observations of post-larvae abundance in the western Channel. The particle tracking module was coupled online to the hydrodynamic model MARS (Lazure et al. 2009). We used the MARS3D V11.1 with a configuration at 2.5 km spanning an area from northern Portugal to the southern North Sea, as further detailed by Petton et al. (2023; see their Fig. 5). The

model used 40 depth layers in the vertical domain. Atmospheric forcing was provided by the Météo-France model ARPEGE. Daily run-off data from the main rivers were included. Boundary conditions for temperature and salinity were provided by the Mercator PSY2V4 and PSY4v3 re-analysis, for the early and late years simulated, respectively. The Lagrangian module has the same time step as the hydrodynamic model, i.e. approximately 2 min, and a few seconds on the vertical, to resolve vertical mixing based on a non-naive random walk (Ross & Sharples 2004). On the horizontal, a diffusion coefficient of 5 m² s⁻¹ was set for the random walk.

For each simulated year, we initiated the particle distribution based on egg distribution as sampled in May during the PELGAS survey (Doray et al. 2018b) with CUFES (Checkley et al. 1997, Huret et al. 2018). Since the survey could not be conducted in 2020, we used BIOMAN CUFES data for that year. For each of the selected years, 25 000 particles were released on the 15th of every spawning month from April to August (Huret et al. 2018), proportional to the observed horizontal egg distributions derived from each annual survey, and randomly from surface to 20 m depth. Egg specific gravity was specified based on its relationship with surface water density (Huret et al. 2016) and varied throughout egg development following Ospina-Álvarez et al. (2012). Yolk sack larvae had a similar buoyancy as the last egg developmental stage. When total larval length reached 6 mm, larvae started migrating in the vertical domain between the surface and 25 m depth, following observations in the Bay of Biscay (M. Huret unpubl. data). The Lagrangian module was coupled to a bioenergetic dynamic energy budget (DEB) module to simulate the development and growth of anchovy larvae (Gatti et al. 2017). Temperature data used to force the bioenergetics were provided by the hydrodynamic model, while f of the DEB Holling Type II functional response was set to 0.8, which generated an average growth rate that only depended on temperature without considering food limitation. Since zooplankton concentrations and interannual variability remain poorly validated in biogeochemical models, we made that choice to avoid spurious growth or mortality effects. Hence, interannual and seasonal variability considered with our dispersal model arose solely from circulation and temperature and not food availability.

Larval drift and bioenergetics were influenced by many processes, many of which were associated with significant uncertainties. In addition, fecundity is variable throughout the spawning season but could not be quantified here. Therefore, we included a set of

constraints, with the aim of providing a more complete understanding of the biophysical factors driving the connectivity between the Bay of Biscay and the English Channel, and eventually to be able to draw more robust and realistic conclusions. First, we calculated the number of particles ending in the English Channel (north of 48.5° N and east of 5.7° W) after a drift period of 60 d. Since all simulations started with the same number of particles, changes in this result highlighted the effects of seasonal variability in the circulation, and interannual variability in both the circulation and the spatial distribution of spawning. The drift duration of 60 d corresponded to the maximum age at which larvae reached 40 mm standard length in the Bay of Biscay (Aldanondo et al. 2016), estimated to be the length at which European anchovy metamorphose (Ré 1996, La Mesa et al. 2009). Second, the numbers of particles were weighted by the total numbers of eggs, as the sum of densities over the sampled area, observed during the annual surveys in May. Little information was available about the egg densities outside the May survey period, although these were known to vary. For that reason, the third constraint was the application of a spawning curve as derived from Huret et al. (2018; their Fig. 8) to correct the contribution of each month to spawning, with the highest contribution in June, and lowest in April and August. Finally, we only considered the larvae ending in the Channel that reached metamorphosis at age 60 d. Metamorphosis was based on the requirement to reach a specific maturity level provided by the bioenergetic model, which itself depended on each individual's life history (see Gatti et al. 2017). This final constraint was expected to adversely impact larvae with low growth rates due to low temperatures either as a result of having spawned during early months or in colder years. This was included to represent the feature that slow-growing larvae have higher mortality rates.

2.5. Ushant Front position

One of the main oceanographic features of the area is the Ushant Front, which separates stratified waters to the west and mixed waters in the east (Pingree 1975) and runs from the Isle of Ushant (Ouessant) off Brittany across the 'mouth' of the English Channel to the south coast of England. The front forms a potential boundary for planktonic organisms, and although it was considered in the hydrographic model used for the particle tracking, its exact location during the annual autumn survey was explored using the tempera-

ture profiles from the approximately 100 evenly-spaced CTD stations annually sampled during the PELTIC survey (Doray et al. 2021). Stations where the difference between surface and bottom temperature (ΔT) was above 0.5°C were considered stratified, while those with a smaller or no temperature difference were considered vertically mixed (Monterey & Levitus 1997). The front was drawn by interpolating between stations which separated the mixed and stratified waters. Between 2013 and 2016, only data from the northern waters of the English Channel were available due to restricted survey coverage. From 2017, coverage included the whole of the English Channel.

3. RESULTS

3.1. Genetic analysis of population structure (adults)

The total number of alleles per locus ranged from 12 to 40 (mean 25). Summary statistics are presented in Table 2. Multilocus F_{IS} values were significant for all samples except the Irish Sea-1 sample. However, these values were largely due to loci Ee2-508 and Ee2, which reported significant heterozygote deficits in 9 and 10 samples (out of 12), respectively. In the case of Ee2-508, it did conform to HWE in the 2 Biscay offshore samples as well as in Irish Sea-1. No other locus exhibited a heterozygote deficit in more than 2 samples. Linkage disequilibrium tests provided no evidence of linkage between any pair of loci (i.e. a pair of loci yielding significant test results for a number of samples). Global genetic structure as measured by F_{ST} was highly significant (F_{ST} = 0.017; p < 0.0001). Pairwise F_{ST} values supported a clear separation between the Northern (Irish Sea, English Channel, North Sea) and Southern (Biscay and Northern France) adult samples, with the post-larval sample clustering with the Southern group (Fig. 3). Differentiation between the North/Biscay adult groups was also supported by AMOVA (F_{CT} (among groups) = 0.02, p < 0.001; F_{SC} (among samples within groups) = 0.005, p < 0.0001). Global genetic structure as measured by F_{ST} was highly significant (F_{ST} = 0.017; p < 0.0001). The final mtDNA alignment comprised 449 bp and revealed 108 haplotypes. Phylogenetic reconstruction partitioned these haplotypes into 2 highly supported clades (labelled A and B to fit with Zarraonaindia et al. 2012 and Silva et al. 2014) with 76 and 32 haplotypes in clade A and B, respectively (Fig. 4). Overall haplotype diversity was high (h = 0.95) and similar among samples (Table 2). However, the mtDNA reported the same North—South partitioning as the microsatellite
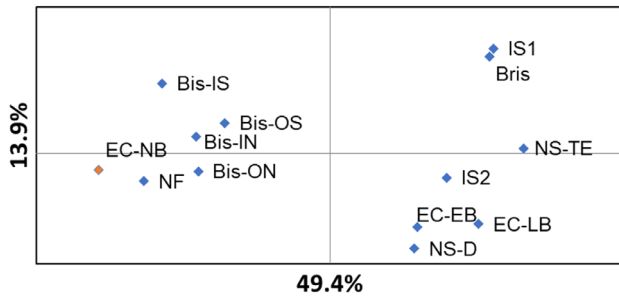
Fig. 3. Principal coordinates analysis of genetic distance between anchovy individuals demonstrating the clear difference between the northern (right) and Biscay (left) groups based on microsatellite analysis. Sample location names are given in Table 2. Juvenile anchovy larvae (EC-NB) are demarcated with an orange diamond

data (Fig. 3), with clade A being almost absent from the northern samples (3%) compared to 50.4% among the southern samples. This translated into highly significant pairwise Φ_{ST} values in all comparisons between regions, while only 1 pairwise value was significant within regions (Table 2). In line with the nuclear patterns, the post-larval sample also exhibited a much higher frequency of mtDNA clade A than found among northern samples (Table 2).
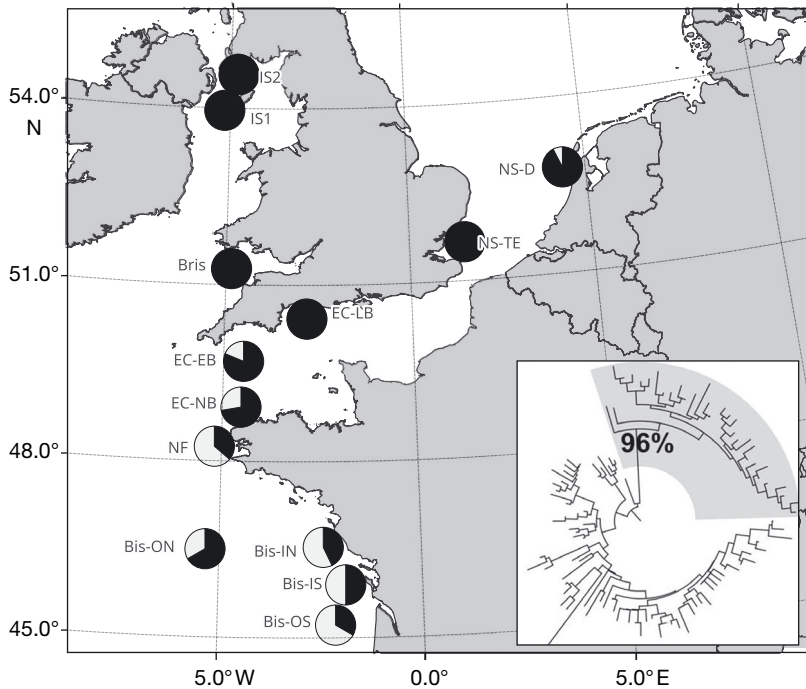

Fig. 4. Northeast Atlantic Ocean, showing genetic sample locations with pie charts denoting relative proportion of the 2 major mtDNA clades (clade A in grey, clade B in black). Inset shows maximum likelihood phylogenetic tree with high bootstrap support (96%) for separation of these clades (clade B sequences shaded). Post-larval sample represented by EC-NB. Further details of genetic sampling locations (including abbreviations) and associated genetic results are given in Table 2

The various Bayesian clustering analyses unanimously identified $K = 2$ (Fig. 5) as the optimal model (p = 0.99 and nearly zero for all other K-values tested). The pattern of individuals clustering followed the F_{ST}-based analyses in revealing the adults from the 4 Biscay and Northern France sites clustered into 1 group (hereafter 'southern group') while the adults sampled in the Irish Sea/Bristol Channel, English Channel and North Sea sites clustered into the other group (hereafter 'northern group'). The post-larval individuals exhibited a strong membership to the southern group. Similarly, when the post-larval individuals were treated as 'unknown', the vast majority (42 of 48 individuals) were assigned to the southern group by IA tests (adults were pooled into northern and southern reference populations as supported by the other analyses).

3.2. Survey-derived anchovy juvenile and egg distribution

Autumn juvenile anchovy showed a variable distribution for the years included in this study. During the historical period (2008–2010), juvenile anchovy showed coastal (2008) as well as offshore (2009 and particularly 2010) distributions (Fig. 6). More recently, juvenile anchovy distribution was generally higher on the shelf with a hotspot off the Gironde estuary in most years. In 2017 and 2018, the northern-most distribution of juvenile anchovy seemed to be restricted to a narrow coastal strip off Brittany, with no juveniles observed in the western English Channel. In 2019, small numbers of juvenile anchovy were found in the SW of the English Channel, along the north coast of Brittany. It was unclear from the map whether these were connected to the northern Bay of Biscay due to a significant gap in survey coverage (detailed in the caption of Fig. 6). Apart from typical shelf sea distribution in 2020, juvenile anchovy were found further offshore in the north of the Bay of Biscay with significant numbers also in the western English Channel, extending at least 120 nautical miles (n miles) east into the Channel. Anchovy were reported at the easternmost transects of the survey and may therefore have
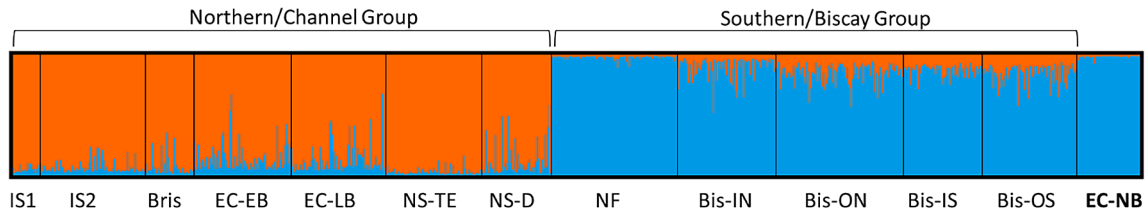
Fig. 5. STRUCTURE barplot (Pritchard et al. 2000) reporting the assignment of individual anchovy specimens (*x*-axis) from different sample location (abbreviations refer to sampling locations, see Table 2), delineated by black lines, under the optimal clustering mode of *K* = 2 based on microsatellite results of anchovy collected during this study in the Northeast Atlantic. Two distinct groups were termed Northern and Biscay. **Bold** sample EC-NB represents the juvenile anchovy from the surface schools. *y*-axis denotes relative contribution of microsatellite to either of 2 clusters, represented by orange and blue colours

extended further east in the English Channel (ICES 2021). Juvenile anchovy densities were lower in 2021 and while found at the northern perimeter of the Bay of Biscay (48°N), none were found in the western English Channel. Both the length range (4.0−9.5 vs. 5.0−10.0 cm), and weighted mean length (4.5 vs. 6.5 cm) of juvenile anchovy in the English Channel was smaller in 2019 compared to 2020 (Fig. 7). In both 2019 and 2020, the juvenile anchovy from the surface schools were distinctly smaller than the anchovy typically encountered during the survey and which included ages 0 to 2 yr old (Fig. 7).
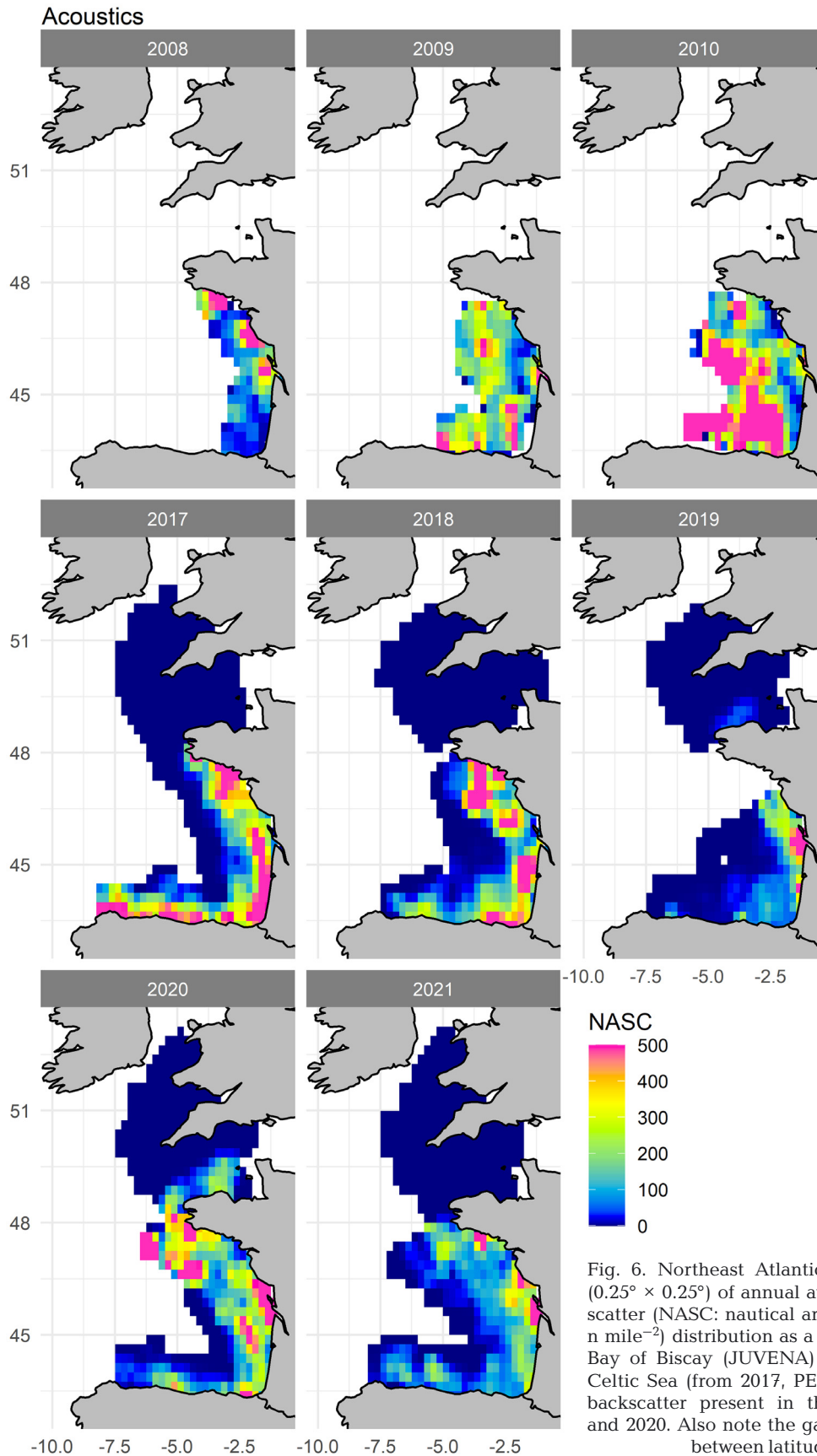
In the early period (2008−2010), spring egg densities (May) were relatively low and were confined to the southern Bay of Biscay (Fig. 8). From 2017, densities were generally higher, with some evidence of spawning activity occurring further north in some years. In 2020, a distinct band of high egg densities suggested peak spawning in May occurred further offshore, whereas in 2021, two parallel bands of spawning were observed, one inshore along the coast and one off the shelf edge (Fig. 8). In 2019, 2020 and 2021, spawning occurred further north than previously observed. In 2010 and 2017, spring coverage included the southwestern English Channel and no anchovy eggs were found. To date, no anchovy eggs or recently hatched larvae have been recorded in ichthyoplankton samples collected during the PELTIC survey in the western English Channel during October.

3.3. Early life stage dispersal model

The larval drift modelling revealed intra- and interannual variability in the connectivity patterns between the yearly egg distribution, as observed during the surveys, and the larval distribution at age 60 d (Fig. 9A). The number of larvae reaching the English Channel at the end of the larval stage generally decreased as the spawning season progressed (Fig. 9A), from 1.6% in April, ~0.6% in May and June, to fewer than 0.2% in July and August (monthly averages across the years). The annual proportion (averaged across spawning months) was lower during the early period (less than 0.02% in 2009−2010) compared to the recent period (1.8 and 1.6% in 2020 and 2021, respectively), although 2008 (0.6%) saw an intermediate proportion. The largest contribution of larvae reaching the Channel was predicted to originate from April and May 2020 spawning times (5.4 and 2.1%, respectively) and from April and June 2021 (3.0 and 2.8%, respectively). All particles reaching the English Channel originated from the northern Bay of Biscay (north of 46°N, Fig. A1 in the Appendix).

After applying the total annual egg production, based on estimates obtained from the surveys, the year 2020 was predicted to contribute about 2 to 4 times more individuals to the Channel compared to 2021 and 2019, respectively (Fig. 9b). When considering the known spawning curve, with a peak in June, then the annual contributions remained almost similar, with 2021 increasing slightly relative to 2020. Contributions in the years 2009 and 2010 were reduced to null since their monthly contribution came from April and May when spawning is low compared to June (Fig. 9c). When considering the larval bioenergetics, with the constraint of reaching the juvenile stage at age 60 d, most larvae made it to the English Channel in 2021. Particularly June-spawned eggs contributed (Fig. 9d) when temperature was more favourable (warmer) for rapid growth compared to earlier in the year. None of the larvae born in April reached the Channel by Day 60 of the juvenile stage (all simulated years). When all constraints were combined, the years 2020 and 2021, and particularly the month of June, contributed the highest number of larvae to the Channel, followed by 2018 and 2019. The early years (2008−2010) contributed none or only negligible numbers of larvae.
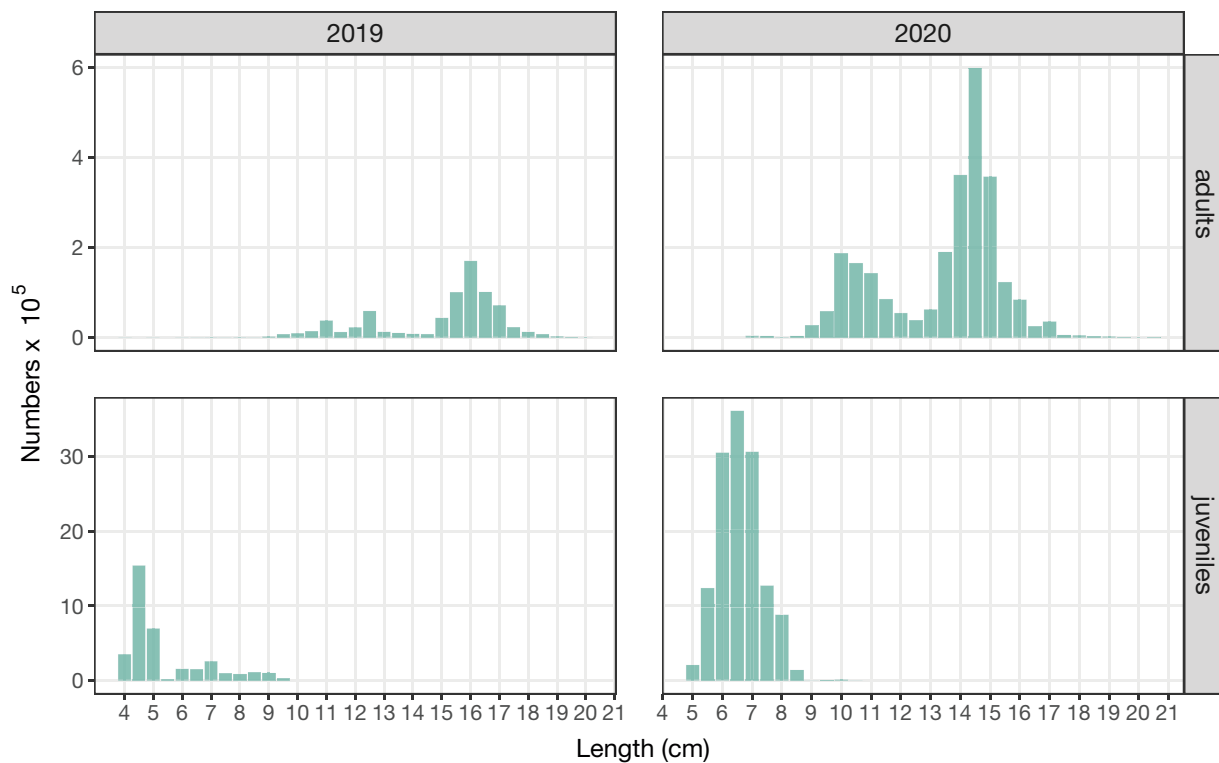
Acoustics

Fig. 6. Northeast Atlantic Ocean, showing grid maps (0.25° × 0.25°) of annual autumn juvenile anchovy backscatter (NASC: nautical area scattering coefficient in m^2 n mile^{-2}) distribution as a proxy for abundance from the Bay of Biscay (JUVENA) to the western Channel and Celtic Sea (from 2017, PELTIC). Note juvenile anchovy backscatter present in the English Channel in 2019 and 2020. Also note the gap in survey coverage in 2019, between latitudes ~46.5 and 48° N

Fig. 7. Length-frequency distribution of anchovy observed during the PELTIC 2019 (left) and 2020 (right) surveys in the western English Channel. Juvenile fish from the distinct surface schools (bottom row) compared to those typically encountered in the survey that consisted of anchovy ages 0—2 (top row)

3.4. Variability in Ushant Front position

Annual October frontal maps derived from temperature profiles collected during the PELTIC surveys showed a consistent position of the Ushant Front in the south of the survey for most of the years (when data were collected at the southern end of the Channel: 2017—2019 and 2021; Fig. 10). The only exception was 2020 when the southern end of the front was positioned much further west. In 2012, the front was extended further west, but this was due to that survey taking place significantly later compared to the rest of the time series (late October to mid-November) and exhibited winter conditions.

4. DISCUSSION

4.1. Juvenile anchovy surface schools in the English Channel originate from the Bay of Biscay

This study aimed to identify the origin of large numbers of juvenile anchovy surface schools ob-served, for the first time, in the southwestern and southern English Channel in 2019 and 2020, and to investigate the mechanisms through which they got there. The absence of anchovy eggs in ichthyoplankton monitoring in the English Channel, the continuity in distribution of anchovy juveniles from the Bay of Biscay into the Channel, as well as the results from particle tracking modelling and from genetic studies all strongly suggest that they originated from the Bay of Biscay. This was the first time this was observed and appeared to present a new scenario in anchovy dynamics in the area, following the finding that previously recorded range expansion was caused by improved survival of remnant spawning populations (Petitgas et al. 2012).

The microsatellite and mtDNA results for adults presented in this study clustered Northeast Atlantic anchovy into 2 spatial coherent groups: a southern group containing specimens from the Bay of Biscay and Brittany, and a northern group containing those from the Irish Sea, Bristol Channel, English Channel and North Sea. This separation readily aligned with results from other genetic studies (Zarraonaindia et al. 2012, Huret et al. 2020). The high level of genetic divergence between the northern and southern groups
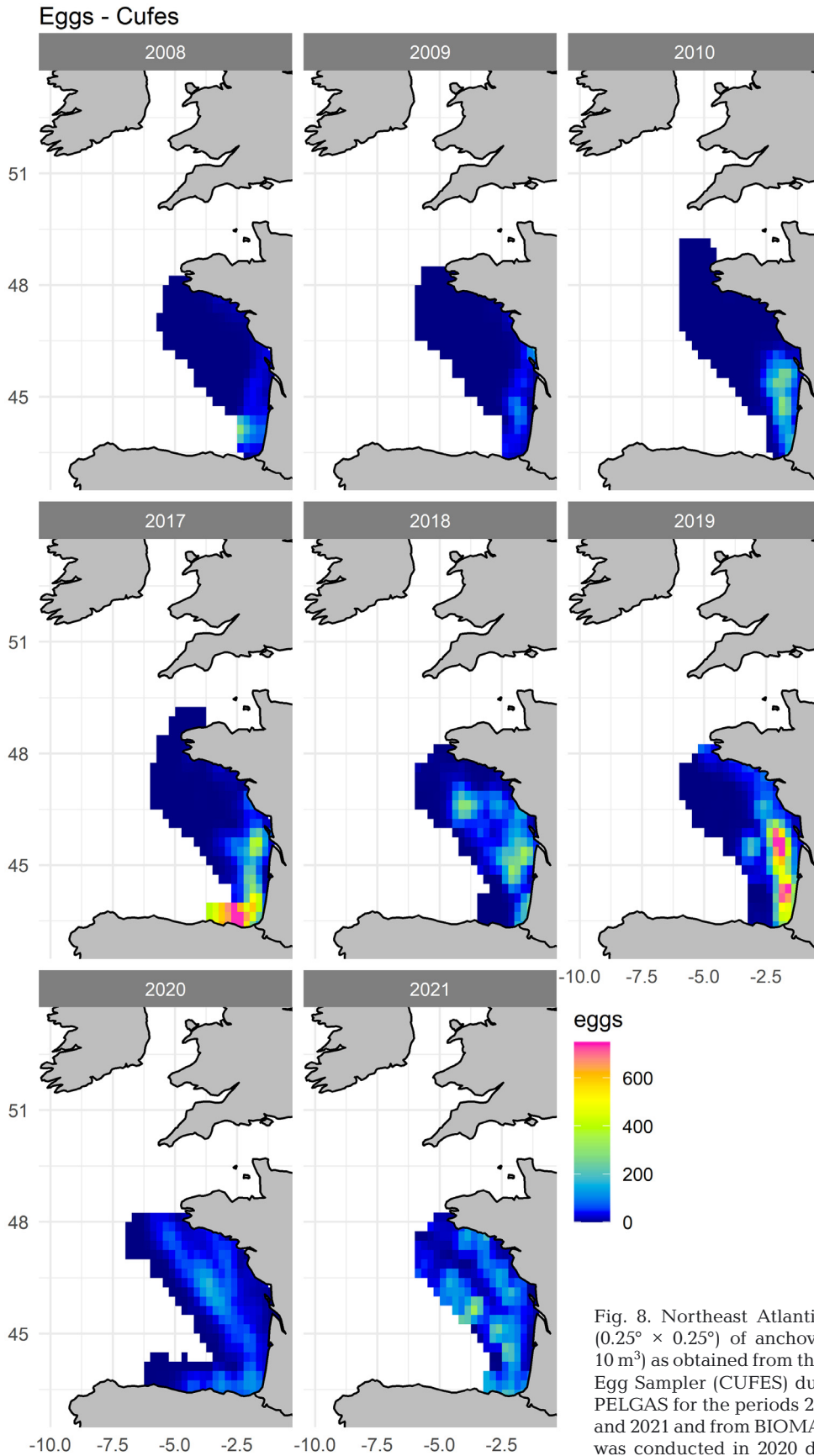
Eggs - Cufes

Fig. 8. Northeast Atlantic Ocean, showing grid maps (0.25° × 0.25°) of anchovy egg densities (numbers per 10 m³) as obtained from the Continuous Underwater Fish Egg Sampler (CUFES) during the annual spring survey PELGAS for the periods 2008—2010 and from 2017, 2019 and 2021 and from BIOMAN in 2020. No PELGAS survey was conducted in 2020 due to the Covid-19 pandemic
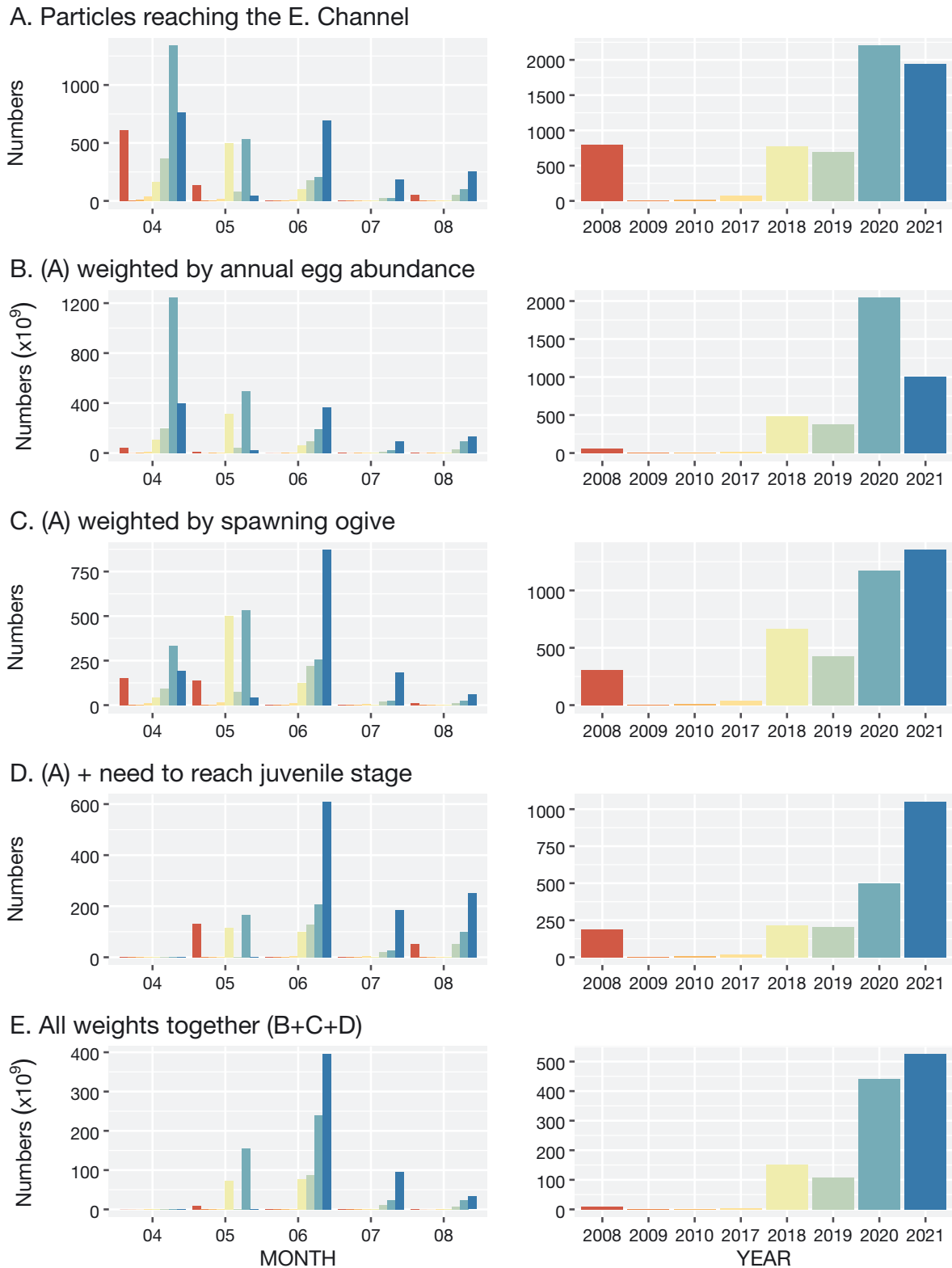
A. Particles reaching the E. Channel

B. (A) weighted by annual egg abundance

C. (A) weighted by spawning ogive

D. (A) + need to reach juvenile stage

E. All weights together (B+C+D)

Fig. 9. Monthly (left) and annual (right) numbers of particles reaching the English Channel (north of 48.5° N and east of 5.7° W) after a drift period of 60 d following release in each month of the spawning period. (A) Raw model output sensu Fig. A1 and (B) with the number of particles weighted by the total number of eggs estimated during the survey in May, (C) by the proportion of spawning among months, (D) only considering particles that reached metamorphosis based on the bioenergetic model, and (E) with all previous weighting and constraints combined. Note that numbers are much higher in B and E because of the weighting by the total egg abundance. Colours on the monthly panels (left) correspond to the years as coloured on the yearly panels (right)
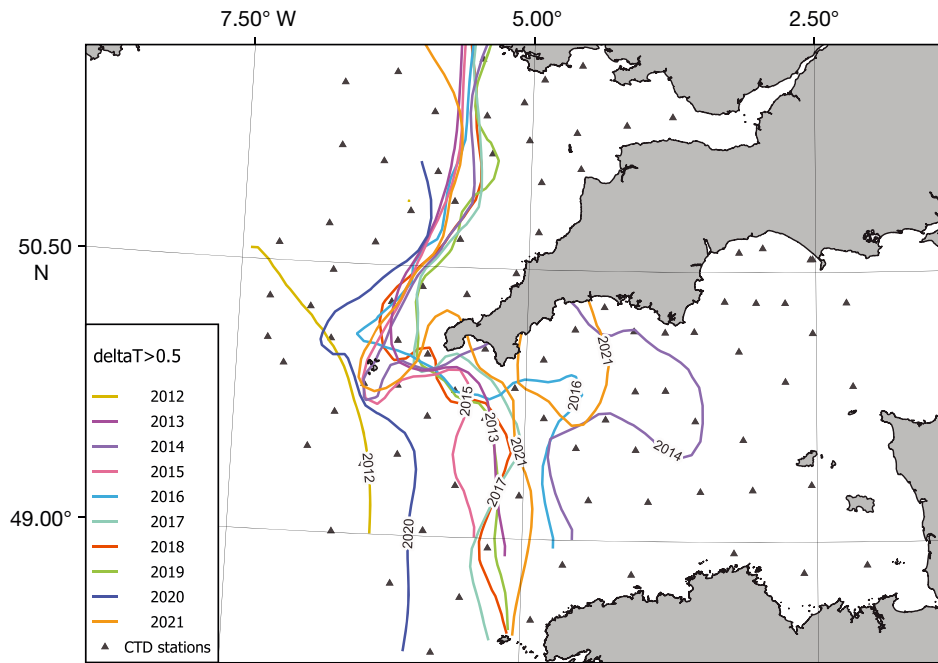
Fig. 10. Northeast Atlantic, showing main Ushant frontal position, colour-coded by year, as derived by interpolating between stations that delineated stratified waters, where the CTD profile exhibited a thermocline, and mixed waters. The water column was considered stratified when the difference between surface and bottom temperature (ΔT) was above 0.5°C (Monterey & Levitus 1997). Note that survey coverage between 2012 and 2016 was restricted to the northern waters of the western English Channel and therefore did not represent the whole front. Triangles represent position of CTD stations

permitted individuals to be robustly assigned. Both STRUCTURE and IA analysis assigned the majority of postlarval samples to the southern group. This detection of larvae of Biscay origin in the Channel suggested that connectivity between the Bay of Biscay and the English Channel has become possible in recent years through larval drift.

This was confirmed by particle tracking modelling conducted during the present study, which suggested that the potential for connectivity increased between the end of the 2000s and the most recent years (2018–2021). It confirmed that previous conditions, represented by 2008–2010, were not conducive to eggs/juveniles reaching the English Channel due to prevailing spawning taking place in the south of the Bay of Biscay. Some northern spawning activity was observed in 2008, and some eggs were predicted to reach the Channel. However, total spawning activity that year was very low and most of the larvae reaching the Channel originated in April. This matched previous findings (Petitgas et al. 2012). In contrast, particle tracking modelling based on spawning conditions during recent years (2017–2021) predicted that anchovy larvae were able to reach the Channel, specifically off northern Brittany. Initially, predicted numbers were negligible (2017) and moderate (2018 and 2019), which in part matched the survey observations, with first post-larval anchovy reported in 2019.

In 2020, very high numbers were predicted to arrive in the Channel, which also matched survey observations. Spawning has increased everywhere in the Bay of Biscay as a result of a growing anchovy spawning stock biomass since the early 2010s (ICES 2023). In the most recent years, spawning has also increased substantially in the northern part of the Bay of Biscay in May, the only part that our study suggests connects with the English Channel through larval drift. This northward expansion of the spawning distribution was previously described and related to density-dependent processes under increasing spawning stock biomass (Petitgas et al. 2014, Erauskin-Extramiana et al. 2019). Temperature may have contributed as well, although this is not proven explicitly in this study: 2019 and 2020 were particularly mild, which may have facilitated a temporal (earlier) and spatial (northerly) expansion of the spawning habitat. Forecasted increases in temperature are anticipated to improve conditions for anchovy egg production, and to expand its spawning habitat. Both factors would induce higher egg densities and, under density-dependent processes, will further increase the potential for spawning north in the Bay (Erauskin-Extramiana et al. 2019) and hence connectivity with the English Channel.

Not all model predictions matched survey observations, as moderate and high numbers were predicted

to reach the Channel in 2018 and 2021, respectively, yet no juveniles were encountered during the survey in the English Channel. As in 2020, juveniles were found in 2021 towards the northern boundary of the Bay of Biscay but in much lower densities than in 2020. The discrepancies between modelled and observed juvenile distributions could be due to several reasons. The dispersal model assumed annual spawning locations throughout the season were as observed during May surveys of that year. While the total spatial range is likely not to change within a year, seasonal shifts in dominant spawning activity may occur and could have influenced the connectivity. Also, the 2 acoustic surveys monitoring juvenile anchovy only provide a snapshot of a few weeks, and a slight alteration in survey timing or hydrography may result in any anchovy influx being missed. This may be exacerbated by the fact that some post-larvae may have developed swimming ability which was not considered by the drift model. Another possibility is that the juveniles continued to drift north rather than entering the channel. This could be caused by subtle oceanographic features that were not captured (accurately) in the hydrographic model which underpinned the dispersal model. The Ushant Front, situated across the mouth of English Channel, may act as a barrier, limiting planktonic (surface) organisms, including post-larval anchovy, to pass. This could explain the observation that most larvae were observed in the Channel in 2020 when the Ushant Front was extended much further west than in other years. Also, the presence of Bay of Biscay genetic features in the Bristol Channel sample suggested that some anchovy may have previously drifted north past the frontal barrier at the entrance of the English Channel. The Ushant Front, which, like other fronts, is itself likely to be affected by climate change (Ferrari 2011), and its potential role in the connectivity of anchovy between the 2 areas, requires further examination.

4.2. When were these anchovy juveniles born?

The particle tracking model results suggested it was primarily spawning in June and to a lesser extent May and July, which contributed eggs that reached the English Channel. This could not be confirmed by survey data, as no detailed age information was available for the juvenile anchovy sampled. However, the mean size of the juvenile anchovy of 4.5 cm (2019) and 6.5 cm (2020) suggested that fish were between 40 and 70 and between 60 and 80 d old, respectively (Aldanondo et al. 2016). Given their capture date

(between 9 and 18 October in both years) and local conditions, this would suggest these fish were born between late July and late August. Within the Bay of Biscay, Aldanondo et al. (2016) estimated the hatch-date of autumn juveniles to range from mid-June to mid-August with a peak in mid-July. This was at least 1 mo later than the spawning peak previously reported to be in May—June (Motos et al. 1996, Huret et al. 2018). The length distribution of the juvenile anchovy in the present study also suggested that their birth date was later than June as estimated by the larval drift experiment. This apparent inconsistency across several studies could be explained if late (post-June) spawned individuals have improved survivability, compared to those originating from the peak spawning period in June.

4.3. What does the future hold for these Biscay juveniles in the Channel?

It is at this stage not known whether the juvenile anchovy that reach the English Channel settle there or return to the Bay of Biscay. Their survival is likely dependent on the genomic properties which will influence the ability to adapt to northern conditions. The transcriptome study by Montes et al. (2016) reported evidence of adaptive divergence between offshore spawning ecotypes from Bay of Biscay and northern inshore spawning ecotypes. This points to selection differences between the regional groups, and could suggest that Bay of Biscay specimens are not able to survive or mix with those from the North Sea. If they do stay and integrate in the northern population, it would alter what has been a prolonged localised restriction on dispersal and gene flow between both regions, and could be observed in future adult genetic samples. The current distinct genetic signatures of the 2 populations (Petitgas et al. 2012, Huret et al. 2020, this study) suggest that this has not happened yet, although the reference samples in this study were collected several years prior to the post-larval samples. In addition to the genetic differences between Bay of Biscay and northern anchovy, there is some evidence that the growth rates of the 2 populations are different (Menu et al. 2023).

4.4. What are the possible implications?

Changes in species distribution can have significant implications for the management of the stock, for example through misalignment with monitoring sur-

vey coverage and fishing effort. For anchovy in the Bay of Biscay, a survey-derived recruitment index was a key contributor to improved assessment of this short-lived species after its crash in the early 2000s (Boyra et al. 2013, Uriarte et al. 2023). The presence of significant juvenile anchovy biomass outside the original survey area (11.4% sensu ICES 2021), as observed in 2020, could therefore adversely impact the accuracy of the index with risks to the stock and the fishery. Also, while catches in the English Channel and southern North Sea have thus far been opportunistic and relatively low, a continued increase in anchovy biomass in the region may attract new, more targeted fisheries. Any possible integration of the Bay of Biscay stock with northern anchovy, as discussed above, would further challenge the management of the spawning populations.

There are also potential ecological implications of distributional shifts. Several other small pelagic fish species reside in this area, and the introduction of significant biomass of a generalist planktivorous species like anchovy (Raab et al. 2011, Patel et al. 2023) may alter the trophodynamics through competition or predation on eggs and larvae (Plirú et al. 2012). Juveniles can have particularly large impacts on prey due to their high densities and high mass-specific rates of feeding (Peck et al. 2021 and references therein). Influx of anchovy juveniles such as reported in this study could therefore cause local food limitation. This would adversely affect local autumn-spawning planktivorous fish such as sardine (Coombs et al. 2010), which rely on productivity towards the end of the plankton growing season for larval-stage winter survival (Capuzzo et al. 2022). Changes in the community can alter predator–prey relationships, and ultimately modify entire food webs (Edwards & Richardson 2004). Like other small pelagic fish, anchovy plays a pivotal ecological role as a mid-trophic species in the marine environment, channelling energy from lower trophic levels to top predators. While not necessarily linked to anchovy, changes in some predator distributions have been reported in the area in recent years. Bluefin tuna *Thunnus thynnus* reappeared in the English Channel in 2014 after decades of absence, and increases in prey abundance are likely to have contributed (Horton et al. 2021). Anchovy is also a favoured prey of the Critically Endangered Balearic shearwater *Puffinus mauretanicus*. The species has seen a northwards postbreeding range expansion into the Celtic Sea, although no direct link was found with prey distribution (Phillips et al. 2021).

Changes in biogeography and abundance are just some of the potential impacts of climate change on biota, which also include changes in phenology and body size (Edwards & Richardson 2004, Perry et al. 2005, Dulvy et al. 2008, Simpson et al. 2011, Cheung et al. 2013). Understanding the mechanisms underlying these dynamics is essential to predict future human influences on biodiversity and guide conservation responses. For anchovy in the Northeast Atlantic Ocean, after more than half a century of limited change in distribution at the northern boundary, 2 such processes, both causing poleward movement, have now been described. (1) Petitgas et al. (2012) demonstrated that observed northward anchovy range expansion from the mid-1990s was a result of climate-driven improved survival of northern remnant spawning populations. (2) In this study, we report a new scenario, observed just over 2 decades later, and have provided evidence that a density-dependent-driven change in spatio-temporal spawning patterns has enabled early life stages to expand their normal distribution by more than 100 n miles. The present study has highlighted that the range dynamics of a taxon at the edge of its distribution is complex and may be due to environmental factors, biotic interactions, human impact and species' life histories.

LITERATURE CITED

Aldanondo N, Cotano U, Goikoetxea N, Boyra G, Ibaibarriaga L, Irigoien X (2016) Interannual differences in growth and hatch-date distributions of early juvenile European anchovy in the Bay of Biscay: implications for recruitment. Fish Oceanogr 25:147–163

Alheit J, Pohlmann T, Casini M, Greve W and others (2012) Climate variability drives anchovies and sardines into the North and Baltic Seas. Prog Oceanogr 96:128–139

Armstrong MJ, Dickey-Collas M, McAliskey M, McCurdy WJ, Burns CA, Peel JAD (1999) The distribution of anchovy *Engraulis encrasicolus* in the northern Irish Sea from 1991 to 1999. J Mar Biol Assoc UK 79:955–956

Aurich HJ (1953) Verbreitung und Laichverhältnisse von

Sardelle und Sardine in der südöstlichen Nordsee und ihre Veränderungen als Folge der Klimaänderung. Helgol Wiss Meeresunters 4:175−204

Beare DJ, Burns F, Greig A, Jones EG and others (2004a) Long-term increases in prevalence of North Sea fishes having southern biogeographic affinities. Mar Ecol Prog Ser 289:264−278

Beare DJ, Burns F, Jones E, Peach K and others (2004b) An increase in the abundance of anchovies and sardines in the north-western North Sea since 1995. Glob Change Biol 10:1209−1213

Boddeke R, Vingerhoed B (1996) The anchovy returns to the Wadden Sea. ICES J Mar Sci 53:1003−1007

Boyce DG, Lewis MR, Worm B (2010) Global phytoplankton decline over the past century. Nature 466:591−596

Boyra G, Martínez U, Cotano U, Santos M, Irigoien X, Uriarte A (2013) Acoustic surveys for juvenile anchovy in the Bay of Biscay: abundance estimate as an indicator of the next year's recruitment and spatial distribution patterns. ICES J Mar Sci 70:1354−1368

Boyra G, Pena M, Cotano U, Irigoien X, Rubio A, Nogueira E (2016) Spatial dynamics of juvenile anchovy in the Bay of Biscay. Fish Oceanogr 25:529−543

Bueno-Pardo J, Petitgas P, Kay S, Huret M (2020) Integration of bioenergetics in an individual-based model to hindcast anchovy dynamics in the Bay of Biscay. ICES J Mar Sci 77:655−667

Capuzzo E, Wright S, Bouch P, Collingridge K and others (2022) Variability in structure and carbon content of plankton communities in autumn in the waters southwest of the UK. Prog Oceanogr 204:102805

Checkley DM Jr, Ortner PB, Settle LR, Cummings SR (1997) A continuous, underway fish egg sampler. Fish Oceanogr 6:58−73

Cheung WWL, Sarmiento JL, Dunne J, Frölicher TL and others (2013) Shrinking of fishes exacerbates impacts of global ocean changes on marine ecosystems. Nat Clim Change 3:254−258

Coombs SH, Halliday NC, Conway DVP, Smyth TJ (2010) Sardine (*Sardina pilchardus*) egg abundance at station L4, Western English Channel, 1988−2008. J Plankton Res 32:693−697

Doray M, Hervy C, Huret M, Petitgas P (2018a) Spring habitats of small pelagic fish communities in the Bay of Biscay. Prog Oceanogr 166:88−108

Doray M, Petitgas P, Romagnan JB, Huret M and others (2018b) The PELGAS survey: ship-based integrated monitoring of the Bay of Biscay pelagic ecosystem. Prog Oceanogr 166:15−29

Doray M, Boyra G, van der Kooij J (eds) (2021) ICES survey protocols — manual for acoustic surveys coordinated under the ICES Working Group on Acoustic and Egg Surveys for Small Pelagic Fish (WGACEGG). ICES Techniques in Marine Environmental Sciences Vol 64

Dulvy NK, Rogers SI, Jennings S, Stelzenmuller V, Dye SR, Skjoldal HR (2008) Climate change and deepening of the North Sea fish assemblage: a biotic indicator of warming seas. J Appl Ecol 45:1029−1039

Edwards M, Richardson AJ (2004) Impact of climate change on marine pelagic phenology and trophic mismatch. Nature 430:881−884

Erauskin-Extramiana M, Alvarez P, Arrizabalaga H, Ibaibarriaga L and others (2019) Historical trends and future distribution of anchovy spawning in the Bay of Biscay. Deep Sea Res II 159:169−182

Evanno G, Regnaut S, Goudet J (2005) Detecting the number of clusters of individuals using the software STRUCTURE: a simulation study. Mol Ecol 14:2611−2620

Excoffier L, Lischer HEL (2010) Arlequin suite ver 3.5: a new series of programs to perform population genetics analyses under Linux and Windows. Mol Ecol Resour 10:564−567

Excoffier L, Smouse PE, Quattro JM (1992) Analysis of molecular variance inferred from metric distances among DNA haplotypes — application to human mitochondrial DNA restriction data. Genetics 131:479−491

Ferrari R (2011) A frontal challenge for climate models. Science 332:316−317

Gatti P, Petitgas P, Huret M (2017) Comparing biological traits of anchovy and sardine in the Bay of Biscay: a modelling approach with the Dynamic Energy Budget. Ecol Modell 348:93−109

Goudet J (1995) FSTAT (Version 1.2): a computer program to calculate *F*-statistics. J Hered 86:485−486

Goudet J, Raymond M, deMeeus T, Rousset F (1996) Testing differentiation in diploid populations. Genetics 144:1933−1940

Hall TA (1999) BioEdit: a user-friendly biological sequence alignment editor and analysis program for Windows 95/98/NT. Nucleic Acids Symp Ser 41:95−98

Horton TW, Block BA, Davies R, Hawkes LA and others (2021) Evidence of increased occurrence of Atlantic bluefin tuna in territorial waters of the United Kingdom and Ireland. ICES J Mar Sci 78:1672−1683

Huret M, Petitgas P, Woillez M (2010) Dispersal kernels and their drivers captured with a hydrodynamic model and spatial indices: a case study on anchovy (*Engraulis encrasicolus*) early life stages in the Bay of Biscay. Prog Oceanogr 87:6−17

Huret M, Bourriau P, Gatti P, Dumas F, Petitgas P (2016) Size, permeability and buoyancy of anchovy (*Engraulis encrasicolus*) and sardine (*Sardina pilchardus*) eggs in relation to their physical environment in the Bay of Biscay. Fish Oceanogr 25:582−597

Huret M, Bourriau P, Doray M, Gohin F, Petitgas P (2018) Survey timing vs. ecosystem scheduling: degree-days to underpin observed interannual variability in marine ecosystems. Prog Oceanogr 166:30−40

Huret M, Lebigre C, Iriondo M, Montes I, Estonba A (2020) Genetic population structure of anchovy (*Engraulis encrasicolus*) in North-western Europe and variability in the seasonal distribution of the stocks. Fish Res 229:105619

ICES (2021) Working Group on Acoustic and Egg Surveys for small pelagic fish (WGACEGG; outputs from 2020 meeting) ICES Sci Rep 3:76

ICES (2023) Working group on southern horse mackerel, anchovy and sardine (WGHANSA). ICES Sci Rep 5:67

Kaschner K, Kesner-Reyes K, Garilao C, Segschneider J, Rius-Barile J, Rees T, Froese R (2019) AquaMaps: predicted range maps for aquatic species. https://www.aquamaps.org

La Mesa M, Donato F, Giannetti G, Arneri E (2009) Growth and mortality rates of European anchovy (*Engraulis encrasicolus*) in the Adriatic Sea during the transition from larval to juvenile stages. Fish Res 96:275−280

Landi M, Garoia F, Piccinetti C, Tinti F (2005) Isolation of polymorphic microsatellite loci from the European anchovy, *Engraulis encrasicolus.* Mol Ecol Notes 5:266−268

Lazure P, Garnier V, Dumas F, Herry C, Chifflet M (2009) Development of a hydrodynamic model of the Bay of Biscay. Validation of hydrology. Cont Shelf Res 29: 985–997

Lenoir J, Bertrand R, Comte L, Bourgeaud L, Hattab T, Murienne J, Grenouillet G (2020) Species better track climate warming in the oceans than on land. Nat Ecol Evol 4:1044–1059

Menu C, Pecquerie L, Bacher C, Doray M, Hattab T, van der Kooij J, Huret M (2023) Testing the bottom-up hypothesis for the decline in size of anchovy and sardine across European waters through a bioenergetic modeling approach. Prog Oceanogr 210:102943

Monterey GI, Levitus S (1997) Seasonal variability of mixed layer depth for the world ocean. NOAA Atlas NESDIS 14. US Government Printing Office, Washington, DC

Montero-Serra I, Edwards M, Genner MJ (2015) Warming shelf seas drive the subtropicalization of European pelagic fish communities. Glob Change Biol 21:144–153

Montes I, Zarraonaindia I, Iriondo M, Grant WS and others (2016) Transcriptome analysis deciphers evolutionary mechanisms underlying genetic differentiation between coastal and offshore anchovy populations in the Bay of Biscay. Mar Biol 163:205

Motos L, Uriarte A, Valencia V (1996) The spawning environment of the Bay of Biscay anchovy (*Engraulis encrasicolus* L.). Sci Mar 60:117–140

Nei M (1978) Estimation of average heterozygosity and genetic distance from a small number of individuals. Genetics 89:583–590

Ospina-Álvarez A, Palomera I, Parada C (2012) Changes in egg buoyancy during development and its effects on the vertical distribution of anchovy eggs. Fish Res 117–118: 86–95

Pakaki V, Magoulas A, Kasapidis P (2009) New polymorphic microsatellite loci for population studies in the European anchovy, *Engraulis encrasicolus* (L.). Mol Ecol Resour 9: 1406–1409

Pappalardo AM, Federico C, Sabella G, Saccone S, Ferrito V (2015) A COI nonsynonymous mutation as diagnostic tool for intraspecific discrimination in the European anchovy *Engraulis encrasicolus* (Linnaeus). PLOS ONE 10:e0143297

Patel R, Roy S, Capuzzo E, van der Kooij J (2023) Seasonality of diet overlap among small pelagic fish in the waters southwest of the UK. Mar Ecol Prog Ser 708:101–123

Peck MA, Alheit J, Bertrand A, Catalán IA and others (2021) Small pelagic fish in the new millennium: a bottom-up view of global research effort. Prog Oceanogr 191:102494

Perry AL, Low PJ, Ellis JR, Reynolds JD (2005) Climate change and distribution shifts in marine fishes. Science 308:1912–1915

Petitgas P, Alheit J, Peck MA, Raab K and others (2012) Anchovy population expansion in the North Sea. Mar Ecol Prog Ser 444:1–13

Petitgas P, Doray M, Huret M, Massé J, Woillez M (2014) Modelling the variability in fish spatial distributions over time with empirical orthogonal functions: anchovy in the Bay of Biscay. ICES J Mar Sci 71:2379–2389

Petton S, Garnier V, Caillaud M, Debreu L, Dumas F (2023) Using the two-way nesting technique AGRIF with MARS3D V11.2 to improve hydrodynamics and estimate environmental indicators. Geosci Model Dev 16: 1191–1211

Phillips JA, Banks AN, Bolton M, Brereton T and others (2021) Consistent concentrations of critically endangered Balearic shearwaters in UK waters revealed by at-sea surveys. Ecol Evol 11:1544–1557

Pingree RD (1975) The advance and retreat of the thermocline on the continental shelf. J Mar Biol Assoc UK 55: 965–974

Pinsky ML, Selden RL, Kitchel ZJ (2020) Climate-driven shifts in marine species ranges: scaling from organisms to communities. Annu Rev Mar Sci 12:153–179

Plirú A, van der Kooij J, Engelhard GH, Fox CJ, Milligan SP, Hunter E (2012) Feeding behaviour, selective predation and daily egg consumption rates by sprat. ICES J Mar Sci 69:1019–1029

Pörtner HO, Peck MA (2010) Climate change effects on fishes and fisheries: towards a cause-and-effect understanding. J Fish Biol 77:1745–1779

Pritchard JK, Stephens M, Donnelly P (2000) Inference of population structure using multilocus genotype data. Genetics 155:945–959

Raab K, Nagelkerke LAJ, Boerée C, Rijnsdorp AD, Temming A, Dickey-Collas M (2011) Anchovy *Engraulis encrasicolus* diet in the North and Baltic Seas. J Sea Res 65: 131–140

Ratnarajah L, Abu-Alhaija R, Atkinson A, Batten S and others (2023) Monitoring and modelling marine zooplankton in a changing climate. Nat Commun 14:564

Raymond M, Rousset F (1995) GENEPOP (VERSION-1.2) — population genetics software for exact tests and ecumenicism. J Hered 86:248–249

Ré P (1996) Anchovy spawning in the Mira estuary (southwestern Portugal). Sci Mar 60:141–153

Ross O, Sharples J (2004) Recipe for 1-D Lagrangian tracking models in space varying diffusivity. Limnol Oceanogr Methods 2:289–302

Santos M, Uriarte A, Boyra G, Ibaibarriaga L (2018) Anchovy DEPM surveys 2003–2012 in the Bay of Biscay (Subarea 8): BIOMAN survey series. In: Massé J, Uriarte A, Angélico MM, Carrera P (eds) Pelagic survey series for sardine and anchovy in ICES subareas 8 and 9 — towards an ecosystem approach. ICES Coop Res Rep 332

Santos M, Uriarte A, Ibaibarriaga L, Motos L (2023) BIOMAN survey. AZTI. https://doi.org/10.57762/N22G-WQ88

Schickele A, Goberville E, Leroy B, Beaugrand G, Hattab T, Francour P, Raybaud V (2021) European small pelagic fish distribution under global change scenarios. Fish Fish 22:212–225

Silva G, Lima FP, Martel P, Castilho R (2014) Thermal adaptation and clinal mitochondrial DNA variation of European anchovy. Proc R Soc B 281:20141093

Simpson SD, Jennings S, Johnson MP, Blanchard JL, Schön PJ, Sims DW, Genner M (2011) Continental shelf-wide response of a fish assemblage to rapid warming of the sea. Curr Biol 21:1565–1570

Tamura K, Stecher G, Peterson D, Filipski A, Kumar S (2013) MEGA6: Molecular Evolutionary Genetics Analysis Version 6.0. Mol Biol Evol 30:2725–2729

Townhill BL, Couce E, Tinker J, Kay S, Pinnegar JK (2023) Climate change projections of commercial fish distribution and suitable habitat around north western Europe. Fish Fish 24:848–862

Uriarte A, Ibaibarriaga L, Sánchez-Maroño S, Abaunza P and others (2023) Lessons learnt on the management of short-lived fish from the Bay of Biscay anchovy case study: sat-

isfying fishery needs and sustainability under recruitment uncertainty. Mar Policy 150:105512

Winnepenninckx B, Backeljau T, De Wachter R (1993) Extraction of high molecular weight DNA from mollusks. Trends Genet 9:407

Woodson CB, McManus MA, Tyburczy JA, Barth JA and others (2012) Coastal fronts set recruitment and connectivity patterns across multiple taxa. Limnol Oceanogr 57: 582−596

Zarraonaindia I, Iriondo M, Albaina A, Pardo MA and others (2012) Multiple SNP markers reveal fine-scale population and deep phylogeographic structure in European anchovy (*Engraulis encrasicolus* L.). PLOS ONE 7:e42201
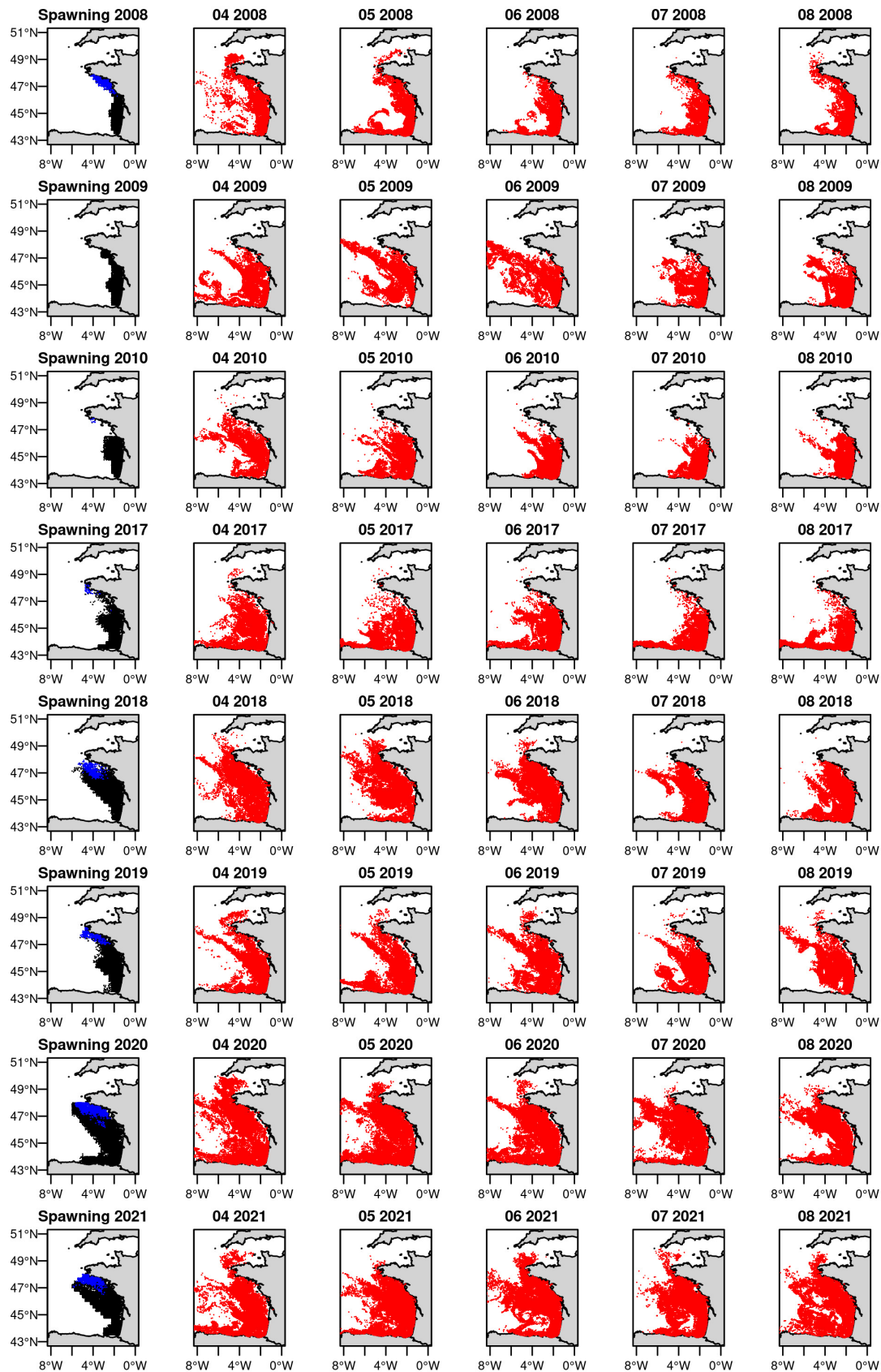
APPENDIX

Fig. A1. Particle tracking results: distribution of 25000 particles on release (left column) based on spring egg distributions observed by year (top to bottom), during PELGAS (2008–2010, 2017–2019, 2021) and BIOMAN (2020) surveys. Columns 2–6 represent modelled end positions of these particles after a 60 d drift period when released at the position indicated in column 1, for each month of the spawning season (April to August) in the Bay of Biscay and each simulated year (2008–2010 and 2017–2021). Blue dots in the first column are starting locations of particles reaching the English Channel in the next columns